FEBS Open Bio 5 (2015) 445–453

FEBS openbio

journal homepage: www.elsevier.com/locate/febsopenbio

# Development of reverse genetics for Ibaraki virus to produce viable VP6-tagged IBAV

Eiko Matsuo [a,*], Keiichi Saeki [a], Polly Roy [b], Junichi Kawano [a]

[a] Microbiology & Immunology, Division of Animal Science, Department of Bioresource Science, Graduate School of Agricultural Science, Kobe University, 1-1, Rokkodai, Nada-ku, Kobe-city 657-8501, Japan

[b] Department of Pathogen Molecular Biology, Faculty of Infectious and Tropical Diseases, London School of Hygiene and Tropical Medicine, Keppel Street, London WC1E 7HT, UK

ARTICLE INFO

*Article history:*
Received 15 April 2015
Revised 13 May 2015
Accepted 22 May 2015

*Keywords:*
Ibaraki virus
Epizootic hemorrhagic disease virus
Reverse genetics system
Primary replication
VP6
Viable VP6-tagged virus

ABSTRACT

**Ibaraki virus (IBAV) is a member of the epizootic hemorrhagic disease virus (EHDV) serogroup, which belongs to the *Orbivirus* genus of the *Reoviridae* family. Although EHDV, including IBAV, represents an ongoing threat to livestock in the world, molecular mechanisms of EHDV replication and pathogenesis have been unclear. The reverse genetics (RG) system is one of the strong tools to understand molecular mechanisms of virus replication. Here, we developed a RG system for IBAV to identify the nonessential region of a minor structural protein, VP6, by generating VP6-truncated IBAV. Moreover, several tags were inserted into the truncated region to produce VP6-tagged IBAV. We demonstrated that all VP6-tagged IBAV could replicate in BHK cells in the absence of any helper VP6 protein. Further, tagged-VP6 proteins were first assembled into puncta in cells infected with VP6-tagged IBAV. Our data suggests that, in order to initiate primary replication, IBAV VP6 is likely to accumulate in some parts of infected cells to assemble efficiently into the primary replication complex (subcore).**

© 2015 The Authors. Published by Elsevier B.V. on behalf of the Federation of European Biochemical Societies. This is an open access article under the CC BY-NC-ND license (http://creativecommons.org/licenses/by-nc-nd/4.0/).

## 1. Introduction

Ibaraki virus (IBAV), a strain of the epizootic hemorrhagic disease virus (EHDV) serogroup, belongs to the genus *Orbivirus*, family *Reoviridae*. Despite the fact that IBAV is distinguishable from the eight other serotypes of EHDV, IBAV partially cross-reacts with antiserum against EHDV serotype 2 (EHDV-2) and thus, the virus is now classified as a strain of EHDV-2 [1–3]. EHDV, including IBAV, is transmitted by blood-feeding midges, *Culicoides* spp., and affects wild and domestic ruminants. EHDV is widespread in cervids, especially white-tailed deer, and causes serious disease (epizootic hemorrhagic disease, EHD) with high mortality [4,5]. However, IBAV was first reported as the etiological agent of Ibaraki disease of cattle, which was characterized by fever, anorexia, salivation, deglutitive disorder and occasionally causes miscarriage [6–9]. More recently, some strains of EHDV serotypes 6 and 7 also caused outbreaks in cattle from Turkey, Morocco, the French island of Réunion and Israel, with high morbidity and mortality resulting in significant losses in cattle industry [10–16]. Thus, EHDV now represents an ongoing threat to livestock in the world. Since 2008, EHD has been added to the OIE notifiable disease list (http://www.oie.int/animal-health-in-the-world/oie-listed-diseases-2015/).

Virus particles of orbiviruses, including IBAV, have three consecutive layers of proteins that are organized into two icosahedral capsids, an outer capsid and an inner capsid (core) [17]. The outer capsid is composed of two proteins, VP2 and VP5, which are a receptor-binding protein and a fusion protein, respectively [18]. The core, composed of two major proteins, VP7 and VP3, encloses the three minor enzymatic proteins VP1 (polymerase), VP4 (capping enzyme) and VP6 (ATP-dependent RNA helicase) in addition to viral genome [19–27]. The viral genome consists of ten-segmented linear double-strand RNA (dsRNA), segment 1 to segment 10 in decreasing order of size (S1–S10). In addition to the seven structural proteins described above, the genome also encodes three or four nonstructural proteins (NS1, NS2, NS3 and NS4), which are expressed in infected host cells [28–30].

The replication of orbiviruses, occurs in two stages [31]. In the first stage, the outer capsid is removed shortly after cell entry and the whole core particle is released from the host cell endosome. The ssRNAs from the 10 genomic segments are then

*Abbreviations:* RG, reverse genetics; IBAV, Ibaraki virus; EHDV, epizootic hemorrhagic disease virus; EHD, epizootic hemorrhagic disease; VIB, virus inclusion body

* Corresponding author. Tel./fax.: +81 (0)78 803 5818.
*E-mail address:* eiko_matsuo@amethyst.kobe-u.ac.jp (E. Matsuo).

http://dx.doi.org/10.1016/j.fob.2015.05.006
2211-5463/© 2015 The Authors. Published by Elsevier B.V. on behalf of the Federation of European Biochemical Societies.
This is an open access article under the CC BY-NC-ND license (http://creativecommons.org/licenses/by-nc-nd/4.0/).

repeatedly transcribed by core-associated enzymes within the core compartment and released into the host cell cytoplasm to act as templates for translation, as well as serving as templates for negative strand viral RNA synthesis enzymes [32–34]. Newly synthesized transcripts, released from the cores, initiate the primary replication cycle generating the replicase complex (subcore), which is composed of VP1, VP3, VP4, VP6 and dsRNA [35–40]. In the second stage, VP7 is added onto the VP3 layer to form the stable core particle [35], which subsequently acquires the two outer capsid proteins, VP2 and VP5, to form mature progeny virions prior to virus egress [41,42].

To understand each step of virus infection more in detail, such as dynamic and multi-step viral entry and intercellular transport of viral proteins, viruses and relevant cellular components are chemically or genetically labeled with fluorescent probes [43]. Recently, using a reverse genetics (RG) system of BTV, virus particles were labeled by insertion of tetracysteine tag (TC-tag) into an outer capsid protein, VP2, to visualize virus attachment and uncoating [44]. However, to date, any internal proteins of orbiviruses, including IBAV, have never been labeled despite the discovery of a nonessential region in BTV VP6 for virus replication in tissue culture [45].

In this study, based on other orbiviruses' RG systems [36,40,46–48], we developed IBAV RG system using *in vitro* synthesized ssRNAs from purified core particle (core transcripts) together with mammalian expression vectors for core proteins (VP1, VP3, VP4, VP6 and VP7) and NS2. Using this system, we generated a viable VP6-truncated IBAV. Importantly, the amino acid (aa) sequence of aa position 34–82 in IBAV VP6, which was nonessential for IBAV replication in cell culture system, was not similar to the one in BTV VP6 (the identity: less than 30%). Moreover, insertion of tags, such as a TC-tag, into the truncated region of VP6 showed non-inhibition of virus growth.

## 2. Materials and methods

### 2.1. Cell lines and virus

BSR cells (BHK-21 subclone) were maintained in Dulbecco's modified Eagle's medium (DMEM) (Nacalai tesque) supplemented with 4.0% (vol/vol) fetal bovine serum (FBS) (Hyclone). BHK21A11 cells were newly subcloned from BHK-21 cells (purchased from RIKEN BRC, Cell Bank) and grown in DMEM-4.0% FBS.

IBAV No.2 strain (IBAV-2) was kindly provided by the National Institute of Animal Health (National Agriculture and Food Research Organization). The virus stocks were obtained by infecting BSR or BHK21A11 cells at low multiplicity of infection (MOI) and harvested when 100% cytopathic effect (CPE) was evident. Titers of viral stocks were obtained by plaque assay and expressed as plaque formation units per ml (PFU/ml). Viral stocks were stored at 4 °C.

### 2.2. Purification of IBAV virus and core particles

IBAV virus and core particles were purified using polyethylene glycol (PEG) as described for rotavirus [49,50] with major modifications. Briefly, BSR cells infected with IBAV-2 at an MOI of 0.05 were harvested at 3 days post-infection and mixed with 8.0% (wt/vol) of PEG 8000 (Sigma) and 0.5 M of NaCl. The mixture was incubated for 16 h at 4 °C and centrifuged at 15,000×*g* (average RCF) at 4 °C for 1 h. The pellets were lysed in a chilled IBAV lysis buffer (50 mM Tris–HCl, pH 8.0; 200 mM NaCl; 5 mM EDTA; 0.5% TritonX-100). Nuclei and insoluble cell debris were removed by centrifugation at 1400×*g* at 4 °C for 15 min. For purification of IBAV particles, the lysate was treated with 1.0% (w/v) N-lauroyl sarkosyl at 25 °C for 1 h. For purification of IBAV core particles, the lysate was treated with 40 μg/ml of α-chymotrypsin and 1.0% (w/v) N-lauroyl sarkosyl at 35 °C for 1 h. After removal of aggregations by centrifugation at 6000×*g* at 4 °C for 5 min, the particles were concentrated by centrifugation through a 30% (w/v) sucrose cushion in 20 mM Tris–HCl (pH 8.0) buffer at 15,000×*g* at 4 °C for 1.5 h. The pellets were re-suspended in 20 mM Tris–HCl (pH 8.0).

Proteins from purified viruses and cores were analyzed by denaturing 10% polyacrylamide gel electrophoresis (SDS–PAGE) followed by staining with Coomassie blue R250.

### 2.3. Synthesis and purification of IBAV ssRNA (core transcripts) in vitro

Core transcripts were synthesized and purified as described previously [47] with some modifications. Briefly, 50 μg of IBAV cores were incubated at 30 °C for 5 h in 500 μl of transcription reaction mix (40 mM Tris–HCl, pH 8.0; 50 mM NaCl; 4 mM rATP; 2 mM rGTP; 2 mM rCTP; 2 mM rUTP; 500 μM S-adenosylmethionine; 5 mM dithiothreitol; 8 mM $MgCl_2$; 50 μM $MnCl_2$) supplemented with 0.2 U/μl RNase inhibitor (Takara). Cores were removed by centrifugation at 15,000×*g* at 4 °C for 45 min. The supernatant was collected and incubated with 2 M LiCl at 4 °C for 16 h. Core transcripts were precipitated by centrifugation at 15,000×*g* at 4 °C for 15 min, re-suspended into OPTI-MEM (Life technologies) and purified using a standard phenol/chloroform extraction method, which completely remove the core particles. Purified core transcripts were analyzed by electrophoresis on a 0.8% agarose gel in MOPS buffer in the presence of formaldehyde.

### 2.4. Plasmids and IBAV T7 transcripts

T7 template plasmids for synthesis of IBAV transcripts used in RG system were generated as described previously [46]. Briefly, dsRNA was extracted from purified core particle using standard methods and cDNA from each segment amplified (FLAC). Each segment was cloned and sequenced. A functional cassette was generated that introduced a T7 promoter directly upstream and a restriction enzyme site directly downstream of each genomic segment.

Modification of S9 was generated by site-directed mutagenesis, using the method as described previously [51]. The mutation inserted in each modified T7 S9 plasmid was confirmed by sequencing.

For IBAV RG system, six mammalian expression vectors, pCAG-PIBAV2VP1, pCAG-PIBAV2VP3, pCAG-PIBAV2VP4, pCAG-PIBAV2VP6, pCAG-PIBAV2VP7 and pCAG-PIBAV2NS2, were generated, as described for BTV RG system [37,40]. Each coding region of IBAV-2 S1, S3, S4, S9, S7 and S8, encoding VP1, VP3, VP4, VP6, VP7 and NS2, respectively, was inserted into the mammalian expression vector pCAG-PM [52]. The sequence of the coding region in each expression plasmid was confirmed.

For synthesis of uncapped T7 transcripts, RiboMAX Large Scale RNA Production System-T7 (Promega) was used according to the manufacturer's protocols as described for BTV [37].

### 2.5. Transfection of cells with core transcripts and/or T7 transcript

Confluent BHK21A11 monolayers were transfected first with six mammalian expression plasmids (0.2 μg each), encoding IBAV VP1, VP3, VP4, VP6, VP7 and NS2, followed by the second-transfection at 20 h post first-transfection with 0.5 μg of IBAV core transcripts using Lipofectamine 2000 Reagent (Life technologies) as described previously [40]. At 6 h post second-transfection, the culture medium was replaced with fresh DMEM containing 5% FBS, instead of 1.5-ml overlay consisting of DMEM, 2% FBS, and 1.5% (wt/vol) low

melting agarose. The plates were incubated at 35 °C in 5.5% $CO_2$ for 1–3 days to allow CPE to appear. The virus titer of recovered IBAV in supernatants harvested at 24 h post second-transfection was determined by plaque assay using BHK21A11 cells.

For the synthetic reassortment experiment, 1.0 μg of T7 transcripts were mixed with 1.0 μg of core transcripts and used for transfection of BSR cells at 20 h post first-transfection with six mammalian expression plasmids. At 2 days post second-transfection, supernatants were collected. Reassortant viruses in collected supernatants were plaque-purified twice in BHK21A11 cells and identified by the profile of the genomic dsRNAs.

### 2.6. Virus growth kinetics

For the growth curves of the mutant or control viruses, monolayers of BSR cells or BHK21A11 cells were infected at MOI of 0.01. At 0, 12, 24, 48 and 72 h post-infection, cells and supernatant were harvested together, disrupted by three freeze–thaw cycles and the total titer was determined by plaque assay using BHK21A11 cells.

### 2.7. Detection of tagged VP6 in infected cells

For immunoblotting, BSR cells were infected with VP6-tagged IBAV at MOI of 0.5 and lysed with IBAV lysis buffer at 24 h post-infection. For detection of tagged VP6 proteins by immunoblotting techniques, a rabbit anti-DDDDK polyclonal antibody (MBL) or a rabbit anti-HA polyclonal antibody (MBL) were used. Proteins were visualized using alkaline phosphatase-conjugated goat anti-rabbit immunoglobulin G (IgG) (Sigma) and substrates for alkaline phosphatase (Promega).

For in-cell TC-tag detection, BSR cells were infected with the VP6-tagged IBAV, IBAVd1TC. At 18 h post-infection, TC-tagged VP6 was detected using FlAsH-$EDT_2$ labeling reagent (Life technologies) according to the manufacture's procedures. The fluorescent cells were observed using fluorescence microscopy (KEYENCE, BZ-9000).

For immunofluorescence, BHK21A11 cells were infected with VP6-tagged IBAV, IBAV2d1HA or IBAVd1Flag, at MOI of 0.5. At 2, 7, 24 and 34 h post-infection, cells were washed once with PBS and fixed in 4.0% (wt/vol) paraformaldehyde. The cells were permeabilized in 0.5% (vol/vol) TritonX-100 (Sigma) in PBS. Staining was performed using either rabbit anti-HA antibody or rabbit anti-DDDDK antibody, followed by CF™568 goat anti-rabbit IgG (Biotium). Nuclei were stained by 4′,6-Diamidino-2-Phenylindole (DAPI) (Nacalai tesque) using standard protocol. Fluorescence was observed using fluorescence microscopy (KEYENCE, BZ-9000).

### 2.8. Electron microscopy

Aliquots of purified viruses and cores were absorbed onto Formvar/carbon support film copper 200 mesh grids (Nisshin EM) for 1 min, washed with water, and negatively stained with 2% (w/v) uranyl acetate. The grids were examined under an electron microscope (JEOL, JEM-1400).

## 3. Results

### 3.1. Purification of IBAV core particles and synthesis of in vitro transcripts

For synthesis of core transcripts, IBAV-2 core particles were purified from BSR cells infected with IBAV-2 virus. As a control, virus particles were purified. Purified core particles were detected using electron microscopy (Fig. 1A) and protein composition was verified by 10% SDS–PAGE gel (Fig. 1B). Although some cell debris still remained, IBAV core particles, with 60–65 nm in diameter, were purified well using PEG-precipitation method without ultracentrifugation step.

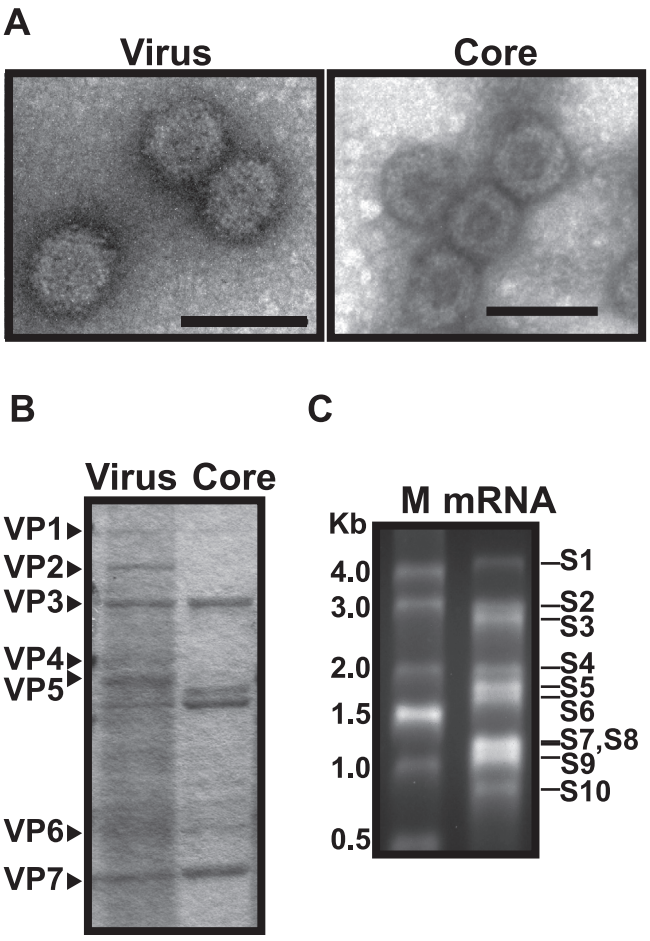


**Fig. 1.** IBAV cores and IBAV core transcripts. (A) Purified IBAV virus (left panel) and IBAV core (right panel) particles stained with 2% uranyl acetate and observed by electron microscopy. The bar represents 100 nm. (B) IBAV virus and core particles purified from BSR cells were resolved by SDS–PAGE. The position of each structural protein is indicated on the left. (C) Profile of IBAV core transcripts (lane mRNA) analyzed by denaturing 1% agarose gel. The numbers on the left indicate the lengths of the marker (lane M) bands in nucleotides. The position of each segment is indicated on the right.

Purified core particles were used for *in vitro* ssRNA synthesis (Fig. 1C). Approximately 20 μg of total core transcripts were synthesized from 25 μg of IBAV core particles.

### 3.2. Recovery of IBAV from core transcripts

To develop a RG system for IBAV, we subcloned BHK-21 cells using a standard limiting-dilution method, as IBAV formed small plaques in BSR cells. BHK21A11 cell line was selected as the cells allowed IBAV-2 to form larger plaques (data not shown). Although the size of plaques differed between BSR cells and BHK21A11 cells, there was no significant difference between the virus replication efficiency in BSR cells versus BHK21A11 cells (data not shown).

In our previous report, we demonstrated the existence of a primary replication cycle in orbivirus infection using a RG system [37,40,48]. Thus, to increase the chances of recovering infectious IBAV from core transcripts, six IBAV plasmids expressing the five core proteins (VP1, VP3, VP4, VP6 and VP7) and NS2, respectively, were generated as described in Materials and Methods. BHK21A11

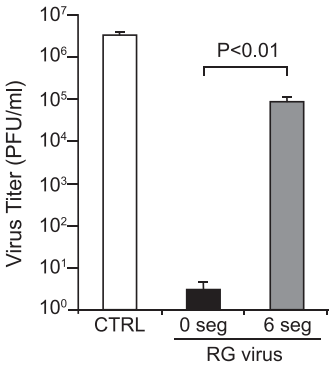


**Fig. 2.** The recovery of IBAV from core transcripts. BHK21A11 cells were transfected with 0.5 μg of IBAV-2 core transcripts either in absence (0 seg) or presence (6 seg) of the first-transfection with six expression plasmids, VP1, VP3, VP4, VP6, VP7 and NS2. As a control (CTRL), BHK21A11 cells were infected with IBAV-2 at MOI of 0.01. The recovery of virus was shown as the amount of infectious virus (PFU/ml) in culture media of transfected cells at 24 h after the second-transfection (RG) or infection (CTRL) (Mean ± SD). The *p*-value was calculated using Student's *t*-distribution.

cells were transfected first with 0.2 μg each of six IBAV plasmids. At 20 h post first-transfection, the cells were subsequently transfected with 0.5 μg of IBAV core transcripts. In parallel, the cells were transfected only once with 0.5 μg of IBAV core transcripts. Only a few plaques, even less plaques than we expected, observed in cells single-transfected with IBAV core transcripts (data not shown). Therefore, the efficiency of virus recovery was determined by the amount of infectious virus in a supernatant of transfected cells, not by the number of plaques formed in transfected cells. Supernatant of each transfected cells was collected at 24 h post second-transfection and the virus titer of IBAV in the supernatant was determined by plaque assay. As a control, BHK21A11 cells were infected with IBAV at MOI of 0.01 and the amount of infectious virus in supernatant of infected cells was determined by plaque assay at 24 h post-infection. Although the titer of IBAV rescued from core transcripts was lower than that of infection with 0.01 MOI of IBAV (Fig. 2, CTRL column versus 6 seg column), the first-transfection with six IBAV plasmids significantly enhanced virus recovery (Fig. 2, 6 seg column versus 0 seg column). Similar results were obtained using BSR cells instead of BHK21A11 cells

**Fig. 3.** Recovery of viable VP6-truncated IBAV from BHK21A11 cells. (A) The secondary structure of IBAV VP6 protein was predicted using Jpred 4 system (http://www.compbio.dundee.ac.uk/jpred/). The aa sequence of IBAV VP6 and the final prediction (Jnet) were shown on the top and second lane, respectively. Numbers indicates aa position. The hidden markov model based prediction (jhmm) and the position specific score matrix based prediction (jpssm) were also shown. The positions of ß-strands and α-helix were indicated as 'E' and 'H', respectively. (B) Genomic dsRNA was purified from infected cells and analyzed by nondenaturing-PAGE. White arrows indicate the position of the corresponding S9 in each VP6-truncated virus. (C) Virus growth kinetics of VP6-truncated viruses IBAVd1 and IBAVd2. Total virus titer was determined by plaque assay at 0, 12, 24, 48, and 72 h post-infection and plotted as PFU/ml in logarithmic scale (Mean ± SD). As a control, cells were infected with WT IBAV-2.

(data not shown). These data suggest that the primary replication cycle is common for all orbiviruses, including IBAV.

### 3.3. Generation of viable VP6-truncated IBAV

Previously, we demonstrated that BTV VP6 possessed two large loops (aa 34–130 and aa 183–231) and that the half of the first loop in BTV VP6 (aa 34–94) was not required for viral replication [45]. The secondary structure prediction of IBAV VP6 (Jpred 4, http://www.compbio.dundee.ac.uk/jpred/) revealed that the region between aa 31 and 130 and between aa192 and 230 are likely to form loops (Fig. 3A) despite the low identity of aa sequence in this region between BTV and IBAV (less than 30%) (data not shown). Thus, it is possible that truncation of half of the first large loop in IBAV VP6 could still allow IBAV replication in normal cells. To identify nonessential regions for virus replication in IBAV VP6, we attempted to generate several VP6-truncated viruses using BHK21A11 cells.

The four deletions were created in T7 S9 transcript. The mutants of S9 lacked nucleotides (nt) sequences coding the first loop, either portions (nt 114–242/aa 34–76, d1; nt 114–260/aa 34–82, d2; nt 114–287/aa 34–91, d3) or complete loop region (nt 114–401/aa 34–129, d4) of VP6. To reduce any detrimental effects on the stability of the core VP6 domain expressed from mutated T7 S9 transcripts, we substituted the deleted region with the15 mer-sequence coding 5 amino acid residues, Gly–Ala–Gly–Ala–Gl y (GAGAG) in frame. The residues, GAGAG, are sufficient to stabilize a VP6 protein structure [45].

We previously reported that recovery efficiency of BTV from T7 transcripts, which were synthesized *in vitro* from T7 plasmids, was considerably lower than that from core transcripts [37,46,47]. In addition, it is normally more difficult to rescue mutated viruses than wild-type virus [37]. Thus, in this study, we used a reassortment method to produce mutated IBAV, instead using a complete T7 system like BTV.

The recovery of viruses containing two mutated S9 RNAs, d1 and d2, was initially screened based on different migration patterns on PAGE gel (Fig. 3B). The identity of S9 mutants was further confirmed using RT-PCR, followed by sequencing (data not shown). The majority of the viruses rescued from BHK21A11 cells was reassortants and consisted of d1 or d2 derived from T7 transcripts. However, IBAV containing other two mutated S9 RNAs, d3 and d4, has never been rescued from BHK21A11 cells in the absence of wild-type VP6.

To further assess the replication capability of VP6-truncated IBAV in normal BHK21A11 cells, the total infectious virus titer (cell-associated and cell-free virus) was calculated at intervals and compared to wild-type IBAV (Fig. 3C). The titers of all VP6-truncated and wild-type IBAV efficiently increased throughout the time course. Although further studies using a complementary cell line expressing wild-type IBAV VP6 is required to determine if deletion between aa 34 and 91 or 129 in VP6 is critical for IBAV replication, at least the region between aa 34 and 82 was likely to be trivial for IBAV replication in BHK cells.

Viable VP6-truncated viruses were further characterized (Fig. 4). The profile of genomic dsRNAs extracted from infected cells in each virus passage (P2, P6, and P11) showed that the truncation was retained in all passaged viruses (Fig. 4A). The presence of the mutation in each passage was confirmed by sequencing the corresponding RT-PCR product (data not shown). Moreover, either an approximately 33 kDa or 32 kDa protein was contained in core particles, which were purified from BSR cells infected with each of

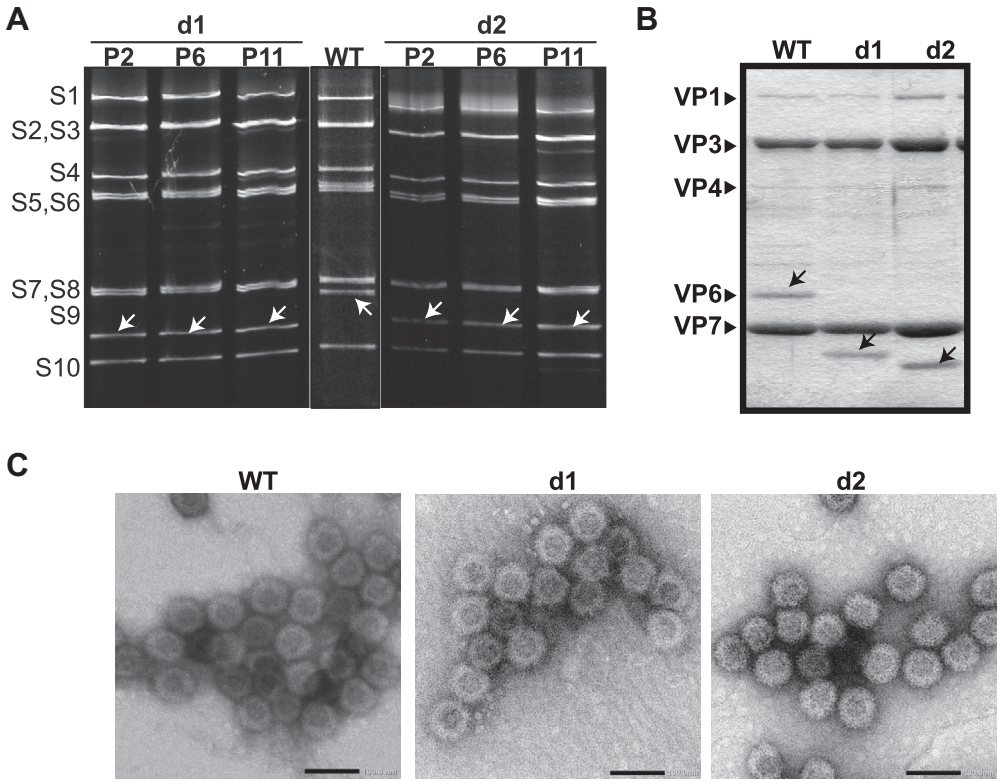


**Fig. 4.** Characterization of VP6-truncated viruses in normal BHK21A11 cells. (A) Each 100 μl of VP6-truncated IBAV plaque-purified twice from BHK21A11 cells were once amplified in BHK21A11 cells (P2), followed by amplification 9 times (P3–P11) in BSR cells. Pattern of genomic dsRNA purified from cells infected with IBAVd1 and IBAVd2 (P2, P6, P11) was analyzed by nondenaturing-PAGE. Position of the corresponding S9 in each VP6-truncated virus is indicated with white arrows. (B) Core particles purified from BSR cells infected with each of P11 IBAV were resolved by SDS–PAGE. Position of the corresponding VP6 in each VP6-truncated virus is indicated with black arrows. (C) Electron microscopy of core particles of each VP6-truncated virus. Bar: 100 nm.

P11 mutated virus (Fig. 4B). As both proteins were not contained in purified wild-type core particle, they were likely to be truncated VP6, sizes of which were estimated as 32.7 kDa and 32.0 kDa, respectively. The data suggests that truncated VP6 was incorporated with the particle. Interestingly, the truncation of VP6 did not affect the size of particles (Fig. 4C).

Together all, these results strongly suggest that truncated VP6 proteins are functional in IBAV replication. In addition, the deletion between aa 34 and 82 in IBAV VP6 does not appear to affect formation of virus particle.

### 3.4. Generation of viable VP6-tagged IBAV

In orbiviruses, since ssRNA sequences of the both ends of each segment, including both non-coding region and a part of coding region, are essential for genome packaging [37], it is impossible to insert tags into the end of the proteins to label the virus particles. However, an unimportant region of VP6, which was partially identified in this study, could allow us to genetically label IBAV particles using RG system by inserting several probes into that region in frame. To determine if the loop region in VP6 could tolerate the insertion of several tags, three VP6-tagged viruses were

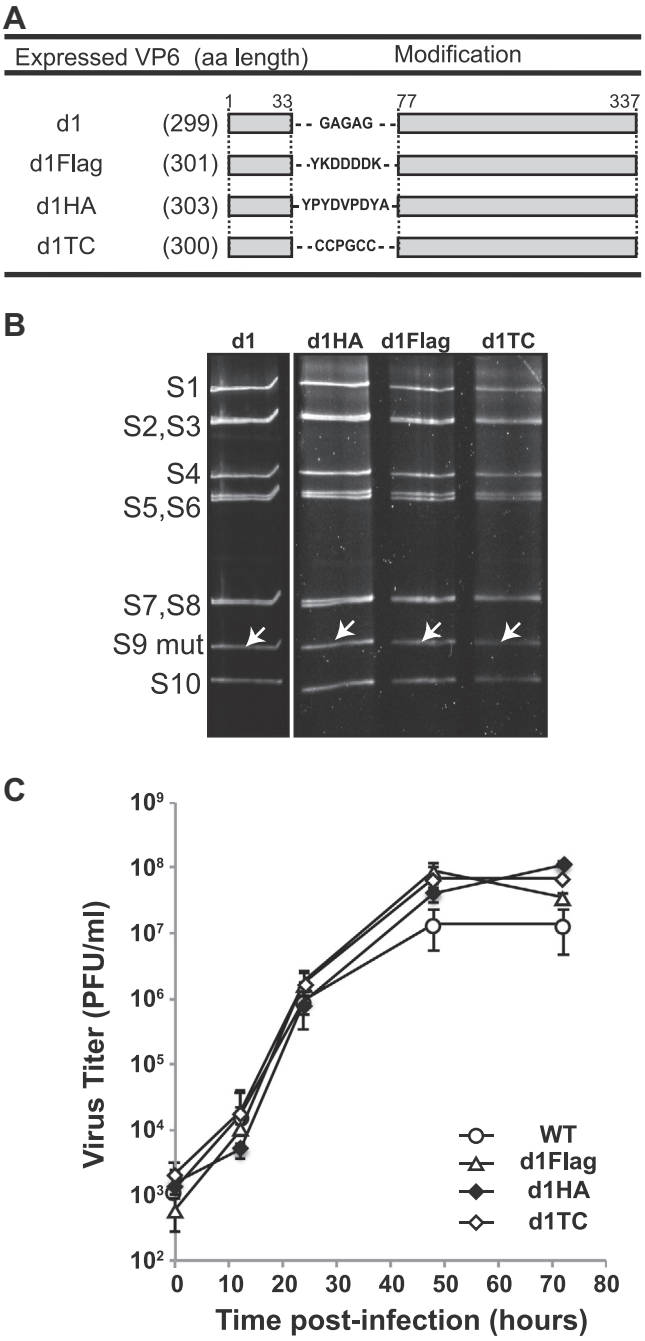


**Fig. 5.** Recovery of viable VP6-tagged IBAV from BHK21A11 cells. (A) Schematic representation of the changes introduced in IBAV VP6. On the left, the name of mutation is indicated. Numbers indicate amino acid positions in VP6 where deletions were introduced. Several amino acid sequences for GAGAG, Flag, HA, and TC were inserted into a truncated region of the first loop. (B) Genomic dsRNA was purified from infected cells and analyzed by nondenaturing-PAGE. White arrows indicate the position of the corresponding S9 in each VP6-tagged virus. (C) Virus growth kinetics of VP6-tagged viruses IBAVd1Flag, HA and TC. Total virus titer was determined by plaque assay at 0, 12, 24, 48, and 72 h post-infection and plotted as PFU/ml in logarithmic scale (Mean ± SD). As a control, cells were infected with WT IBAV-2.

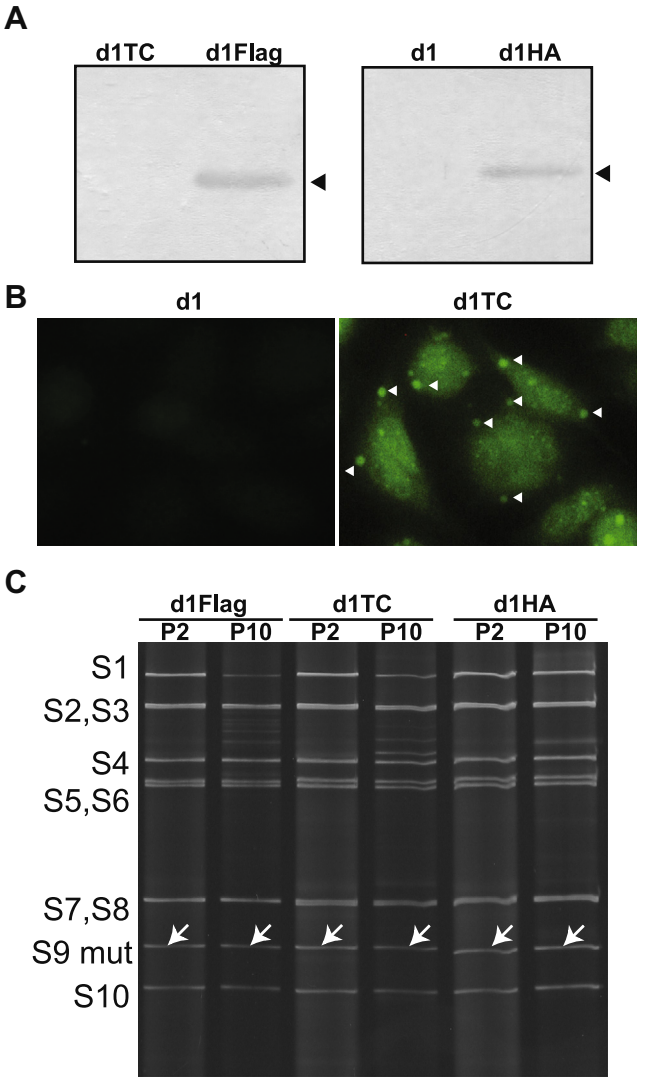


**Fig. 6.** Characterization of VP6-truncated viruses in normal BHK21A11 cells. (A) Either Flag or HA-tagged VP6 were detected in BSR cells infected with VP6-tagged IBAV by immunoblot analysis. As a control, IBAVd1 or IBAVd1TC were infected to the cells. Arrowheads indicate the detected tagged proteins. (B) TC-tagged VP6 was detected in the IBAVd1TC-infected BSR cells using FlAsH-$EDT_2$ labeling reagent. Note that some TC-VP6 proteins were detected as puncta (white arrowheads). (C) After 10 times passage of each VP6-tagged IBAV, pattern of genomic dsRNA purified from cells infected with IBAVd1Flag, HA and TC (P2 and P10) was analyzed by nondenaturing-PAGE. Position of the corresponding S9 in each VP6-tagged virus is indicated with white arrows.

generated by substituting aa position 34–76 of IBAV VP6 with Flag-tag (YKDDDDK), HA-tag (YPYDVPDYA) or TC-tag (CCPGCC) in frame (Fig. 5A). All three VP6-tagged IBAV, IBAVd1Flag, IBAVd1HA and IBAVd1TC, were successfully generated by IBAV RG system using BHK21A11 cells (Fig. 5B).

To further confirm the viability of VP6-tagged IBAV, BHK21A11 cells were infected at MOI of 0.01 with each of VP6-tagged viruses and harvested at 12, 24, 48 and 72 h post-infection. The titers of all VP6-tagged viruses increased throughout the time course, similar to that of the wild-type IBAV (Fig. 5C), suggesting that tagged VP6 was functional in IBAV replication.

Each of tagged VP6 proteins was detected in cells infected with each VP6-tagged virus (Fig. 6A and B). Flag or HA-tagged VP6 with expected size (~33 kDa) were detected by anti-DDDDK antibody and anti-HA antibody, respectively (Fig. 6A) and TC-tagged VP6 was successfully labeled with FlAsH reagent at 18 h post-infection (Fig. 6B). Note that some of TC-tagged VP6 proteins formed puncta. In addition, the incorporation of tagged VP6 with purified IBAV particle was confirmed using antibodies against tags (data not shown).

To access the stability of inserted tags, each VP6-tagged virus was continuously passaged 10 times and dsRNA profiles of passage 2 (P2) and passage 10 (P10) were confirmed (Fig. 6C). The presence of the mutation in each passage was also confirmed by sequencing the corresponding RT-PCR product (data not shown).

### 3.5. Translocation of VP6 in early infection of IBAV

Despite decades of attempts to clarify the actual role of VP6, the exact function of BTV VP6 in BTV biology still remains to be addressed. Our data demonstrated that VP6 with substitution of region between aa 34 and 76 with tags were still functional and could act exactly same as wild-type VP6. Thus, VP6-tagged IBAV could allow us to detect the precise location of VP6 in infected cells, as well as in virus particle.

Interestingly, TC-tagged IBAV formed puncta in infected cells at 18 h post-infection (Fig. 6B). To further confirm if VP6 forms puncta in early infection, BHK21A11 cells were infected with VP6-tagged IBAV and at 2, 7, 24 and 36 h post-infection (Fig. 7). At 7 h post-infection, Flag-tagged VP6 already assembled into puncta, while the proteins were detectable throughout the cytosol at 24 h and 36 h post-infection (Fig. 7A). HA-tagged VP6 also assembled into puncta at 7 h post-infection in BHK21A11 cells (Fig. 7B right panel). The same results were obtained using BSR cells (data not shown). As orbivirus VP6 is likely to be important for assembly of the primary replicase complex [37,40], these data suggest that VP6 may be necessary to be concentrated in cytosol of the infected cells in order to initiate primary replication efficiently.

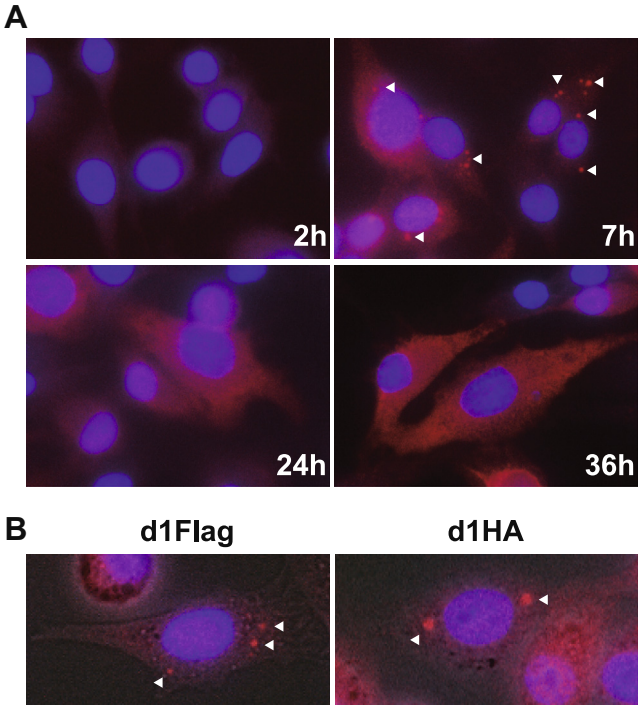


**Fig. 7.** Translocation of tagged VP6 in the infected cells. (A) Flag-tagged VP6 was detected using anti-rabbit DDDDK antibody at 2, 7, 24, and 36 h post-infection with IBAV d1Flag at MOI of 0.5. Nuclei were stained with DAPI. Arrowheads indicate puncta formation of VP6. (B) Magnified images of BHK21A11 cells infected with either IBAVd1Flag (left) or IBAVd1HA (right) at 7 h post-infection. Nuclei were stained with DAPI. Arrowheads indicate puncta formation of VP6. Fluorescent images were merged with bright field images.

## 4. Discussion

Despite the potential for devastating economic impact on the livestock industry, studies on EHDV, including IBAV, replication and pathogenesis have been hampered due to lack of methods for the rescue of infectious virus from cloned nucleic acid (RG system). Therefore, until now, it has not been possible to carry out introduction of targeted mutations into replicating virus genomes. We presented here a method to undertake RG experiments with IBAV. In particular, we first generated viable VP6-tagged IBAV and demonstrated translocation of IBAV VP6 in real IBAV replication.

Our previous studies on replication of orbiviruses, such as BTV and African horse sickness virus (AHSV) [36,37,40], indicated that the primary replication step was common to the replication of all orbiviruses. Our RG data confirmed its existence in EHDV. Although the replication efficiency of IBAV in BHK cells was almost equivalent to that of BTV or AHSV, the recovery efficiency of IBAV RG system was much lower than that of BTV or AHSV RG system. IBAV is less virulent than BTV and AHSV (ie mortality ~20% versus over 70%) [17,53,54]. In addition, most EHDV, including IBAV, cause subclinical infection in cattle [55–57], in which virus replication could be suppressed. Thus, it is possible that some unknown factors, which efficiently initiate primary replication soon after second-transfection of core transcripts, could be lacking in current IBAV RG system. For development of the complete plasmid-based T7 RG system for IBAV, some modification is required. RG system for hepatitis C virus requires enough viral polymerase activity to trigger genome replication [58–61]. Polymerase activity of IBAV may be lower than those of BTV and AHSV.

The truncation of a region between aa 34 and 94 in BTV VP6 still allowed the VP6-truncated BTV to replicate in absence of wild-type VP6 [45]. On the other hand, our data showed that a deletion of a region between aa 34 and 82 in VP6 still allowed VP6-truncated IBAV to replicate in absence of wild-type VP6 but not a deletion of a region between aa 34 and 91 (d3) in the protein. A complementary cell line, BSR-VP6, was used for rescue of VP6-truncated BTV, whereas only normal BHK21A11 or BSR cells were used for rescue in this study. Thus, it is still possible that enough amount of wild-type VP6 could be required only for the first recovery of d3 virus and, once the virus recovered, d3 can replicate in the absence of wild-type VP6. Another possibility is that the essential region in VP6 for IBAV replication could be different from that for BTV replication. Interestingly, aa sequences of the loop regions in VP6 are variable among orbiviruses whereas non-coiled regions in VP6 were highly conserved (Matsuo et al. unpublished data).

This variation of residues in flexible loop might be an important factor to cause differences in initiation of primary replication. Nevertheless, further studies are required to determine whether the failure of d3 recovery was due to lack of essential region in VP6, which includes a region between aa 82 and 91, for IBAV replication or just a technical issue.

VP6-trancated IBAV and VP6-labeled IBAV were likely to replicate even better than wild-type IBAV, especially after 48 h post-infection. The deletion between aa 34 and 82 of VP6 may affect the efficiency of IBAV replication. As well as VP6, a nonstructural protein, NS4, which plays an important role in virus-host interaction, is also encoded in S9 segment [28]. Thus, the partially deletion of VP6 results in a deletion of NS4. Although further studies are required, it is possible that the deletion of either a part of VP6 or NS4 changed the cytotoxicity of mutated IBAV.

Orbivirus, including EHDV, is unique among the *Reoviridae* family in encoding VP6, a protein with nucleoside triphosphatase, RNA binding, and helicase activity *in vitro* [20,25,62]. In addition, we recently reported that BTV VP6 possesses an essential role in primary replication and a plausible role in RNA packaging during core assembly as well [37,40,63]. A nonstructural protein, NS2, is the main component of viral inclusion bodies (VIB) in infected cells where assembly of core particle takes place [64–67]. Thus, it is possible that NS2 interacts with VP6 and maybe other viral proteins to form VIB soon after translated. Together with these facts, VP6 should translocate into VIB in early stage of infection. Our data clearly showed that VP6 protein assembled into puncta, which resembled orbivirus VIB [17], in early stage of IBAV infection. Although further studies, such as co-localization assay with NS2, should be necessary, to initiate the primary replication, IBAV VP6 is likely to first translocate into VIB to assemble into the primary replication complex, subcore.

To date, it has not been possible to determine a precise location of VP6 within the core as inside of the particles were completely occupied with internal virus proteins, including VP6, and genome (Matsuo, Noda, Kawaoka and Roy unpublished data). Our data showed that tagged-VP6 did not affect formation of core particle. However, the truncation of VP6 could make some spaces inside of the particle to allow us to identify each of elements in the core.

Recently, live cell imaging techniques have been developed in several viruses, including BTV [43,44]. Insertion of TC-tag into a putative exposed region in an outer capsid protein of BTV, VP2, successfully made infectious BTV particles visible and detectable at virus binding stage in replication [44]. In this study, using newly developed RG system, we demonstrated the insertion of tags into unimportant region of IBAV VP6 to visualize the localization of VP6 after transcription step. In addition, our data suggested that several tags in VP6 should allow us to visualize the inside of the particle. TC-labeling of outer capsid combined with labeling of core proteins should visualize uncoating step in near future.

Overall, the data presented in this report demonstrate the development of EHDV RG system, particular, the ubiquitous existence of unimportant region in orbivirus VP6. Together with techniques already developed in other orbiviruses, it should be possible to define precisely the mechanisms of the virus replication at a finer level. In addition, our data would contribute to clarify the similarity and differences between orbiviruses and other viruses of family *Reoviridae* in virus replication.

## Author contributions

E.M. conceived and designed the project, carried out all the experimental studies and wrote the paper. P.R. and J.K. corrected the paper. All authors analyzed data, read and approved the final manuscript.

## Acknowledgements

This work was supported by JSPS KAKENHI Grant Numbers 24780285 and partly by a "Fund for the Development of Human Resources in Science and Technology" provided by MEXT, Japan.

## References

[1] Campbell, C.H., Barber, T.L. and Jochim, M.M. (1978) Antigenic relationship of Ibaraki, bluetongue, and epizootic hemorrhagic-disease viruses. Vet. Microbiol. 3, 15–22.
[2] Della-Porta, A.J., Gould, A.R., Eaton, B.T. and McPhee, D.A. (1985) Biochemical characterisation of Australian orbiviruses. Prog. Clin. Biol. Res. 178, 337–345.
[3] Sugiyama, M., Hirayama, N., Sasaki, H., Sugimura, T., Minamoto, N. and Kinjo, T. (1989) Antigenic relationship among strains of Ibaraki virus and epizootic haemorrhagic disease virus studied with monoclonal antibodies. Res. Vet. Sci. 46, 283–285.
[4] Stallknecht, D.E., Luttrell, M.P., Smith, K.E. and Nettles, V.F. (1996) Hemorrhagic disease in white-tailed deer in Texas: a case for enzootic stability. J. Wildl. Dis. 32, 695–700.
[5] Gaydos, J.K., Crum, J.M., Davidson, W.R., Cross, S.S., Owen, S.F. and Stallknecht, D.E. (2004) Epizootiology of an epizootic hemorrhagic disease outbreak in West Virginia. J. Wildl. Dis. 40, 383–393.
[6] Inaba, U. (1975) Ibaraki disease and its relationship to bluetongue. Aust. Vet. J. 51, 178–185.
[7] Ohashi, S., Yoshida, K., Watanabe, Y. and Tsuda, T. (1999) Identification and PCR-restriction fragment length polymorphism analysis of a variant of the Ibaraki virus from naturally infected cattle and aborted fetuses in Japan. J. Clin. Microbiol. 37, 3800–3803.
[8] Omori, T. et al. (1969) Ibaraki virus, an agent of epizootic disease of cattle resembling bluetongue. I. Epidemiologic, clinical and pathologic observations and experimental transmission to calves. Jpn. J. Microbiol. 13, 139–157.
[9] Omori, T., Inaba, Y., Morimoto, T., Tanaka, Y., Kono, M., Kurogi, H. and Matumoto, M. (1969) Ibaraki virus, an agent of epizootic disease of cattle resembling bluetongue. 2. Isolation of virus in bovine cell culture. Jpn. J. Microbiol. 13, 159–168.
[10] Sailleau, C. et al. (2012) Co-circulation of bluetongue and epizootic haemorrhagic disease viruses in cattle in Reunion Island. Vet. Microbiol. 155, 191–197.
[11] Kedmi, M., Van Straten, M., Ezra, E., Galon, N. and Klement, E. (2010) Assessment of the productivity effects associated with epizootic hemorrhagic disease in dairy herds. J. Dairy Sci. 93, 2486–2495.
[12] Kedmi, M., Galon, N., Herziger, Y., Yadin, H., Bombarov, V., Batten, C., Shpigel, N.Y. and Klement, E. (2011) Comparison of the epidemiology of epizootic haemorrhagic disease and bluetongue viruses in dairy cattle in Israel. Vet. J. 190, 77–83.
[13] Yadin, H. et al. (2008) Epizootic haemorrhagic disease virus type 7 infection in cattle in Israel. Vet. Record 162, 53–56.
[14] Cetre-Sossah, C. et al. (2014) Epizootic haemorrhagic disease virus in Reunion Island: evidence for the circulation of a new serotype and associated risk factors. Vet. Microbiol. 170, 383–390.
[15] Temizel, E.M., Yesilbag, K., Batten, C., Senturk, S., Maan, N.S., Clement-Mertens, P.P. and Batmaz, H. (2009) Epizootic hemorrhagic disease in cattle, Western Turkey. Emerg. Infect. Dis. 15, 317–319.
[16] Breard, E., Sailleau, C., Hamblin, C., Graham, S.D., Gourreau, J.M. and Zientara, S. (2004) Outbreak of epizootic haemorrhagic disease on the island of Reunion. Vet. Record 155, 422–423.
[17] Roy, P. (2013) Orbiviruses in: Fields' Virology (Knipe, D.M. and Howley, P.M., Eds.), pp. 1402–1423, Lippincott Williams & Wilkins, Philadelphia, New York, USA.
[18] Zhang, X., Boyce, M., Bhattacharya, B., Schein, S., Roy, P. and Zhou, Z.H. (2010) Bluetongue virus coat protein VP2 contains sialic acid-binding domains, and VP5 resembles enveloped virus fusion proteins. Proc. Natl. Acad. Sci. U.S.A. 107, 6292–6297.
[19] Wehrfritz, J.M., Boyce, M., Mirza, S. and Roy, P. (2007) Reconstitution of bluetongue virus polymerase activity from isolated domains based on a three-dimensional structural model. Biopolymers 86, 83–94.
[20] Stauber, N., Martinez-Costas, J., Sutton, G., Monastyrskaya, K. and Roy, P. (1997) Bluetongue virus VP6 protein binds ATP and exhibits an RNA-dependent ATPase function and a helicase activity that catalyze the unwinding of double-stranded RNA substrates. J. Virol. 71, 7220–7226.
[21] Sutton, G., Grimes, J.M., Stuart, D.I. and Roy, P. (2007) Bluetongue virus VP4 is an RNA-capping assembly line. Nat. Struct. Mol. Biol. 14, 449–451.
[22] Ramadevi, N., Burroughs, N.J., Mertens, P.P.C., Jones, I.M. and Roy, P. (1998) Capping and methylation of mRNA by purified recombinant VP4 protein of bluetongue virus. Proc. Natl. Acad. Sci. U.S.A. 95, 13537–13542.
[23] Nason, E.L., Rothagel, R., Mukherjee, S.K., Kar, A.K., Forzan, M., Prasad, B.V.V. and Roy, P. (2004) Interactions between the inner and outer capsids of bluetongue virus. J. Virol. 78, 8059–8067.
[24] Matsuo, E. and Roy, P. (2011) Bluetongue virus VP1 polymerase activity in vitro: template dependency, dinucleotide priming and cap dependency. PLoS One 6, e27702.
[25] Kar, A.K. and Roy, P. (2003) Defining the structure–function relationships of bluetongue virus helicase protein VP6. J. Virol. 77, 11347–11356.

[26] Grimes, J.M., Burroughs, J.N., Gouet, P., Diprose, J.M., Malby, R., Zientara, S., Mertens, P.P. and Stuart, D.I. (1998) The atomic structure of the bluetongue virus core. Nature 395, 470–478.
[27] Boyce, M., Wehrfritz, J., Noad, R. and Roy, P. (2004) Purified recombinant bluetongue virus VP1 exhibits RNA replicase activity. J. Virol. 78, 3994–4002.
[28] Ratinier, M. et al. (2011) Identification and characterization of a novel non-structural protein of bluetongue virus. PLoS Pathog. 7, e1002477.
[29] Verwoerd, D.W. (1969) Purification and characterization of bluetongue virus. Virology 38, 203–212.
[30] Verwoerd, D.W. and Huismans, H. (1972) Studies on the in vitro and the in vivo transcription of the bluetongue virus genome. Onderstepoort J. Vet. Res. 39, 185–191.
[31] Zarbl, H. and Millward, S. (1983) The reovirus multiplication cycle in: The Reoviridae (Joklik, W., Ed.), Springer, New York.
[32] Huismans, H., van Dijk, A.A. and Els, H.J. (1987) Uncoating of parental bluetongue virus to core and subcore particles in infected L cells. Virology 157, 180–188.
[33] Mertens, P.P., Burroughs, J.N. and Anderson, J. (1987) Purification and properties of virus particles, infectious subviral particles, and cores of bluetongue virus serotypes 1 and 4. Virology 157, 375–386.
[34] Van Dijk, A.A. and Huismans, H. (1988) In vitro transcription and translation of bluetongue virus mRNA. J. Gen. Virol. 69 (Pt 3), 573–581.
[35] Lourenco, S. and Roy, P. (2011) In vitro reconstitution of Bluetongue virus infectious cores. Proc. Natl. Acad. Sci. U.S.A. 108, 13746–13751.
[36] Matsuo, E., Celma, C.C. and Roy, P. (2010) A reverse genetics system of African horse sickness virus reveals existence of primary replication. FEBS Lett. 584, 3386–3391.
[37] Matsuo, E. and Roy, P. (2009) Bluetongue virus VP6 acts early in the replication cycle and can form the basis of chimeric virus formation. J. Virol. 83, 8842–8848.
[38] Roy, P. (2008) Bluetongue virus: dissection of the polymerase complex. J. Gen. Virol. 89, 1789–1804.
[39] Roy, P. (2008) Functional mapping of bluetongue virus proteins and their interactions with host proteins during virus replication. Cell Biochem. Biophys. 50, 143–157.
[40] Matsuo, E. and Roy, P. (2013) Minimum requirements for bluetongue virus primary replication in vivo. J. Virol. 87, 882–889.
[41] Bhattacharya, B., Noad, R.J. and Roy, P. (2007) Interaction between bluetongue virus outer capsid protein VP2 and vimentin is necessary for virus egress. Virol. J. 4, 7.
[42] Roy, P. (1996) Orbivirus structure and assembly. Virology 216, 1–11.
[43] Sun, E., He, J. and Zhuang, X. (2013) Live cell imaging of viral entry. Curr. Opin. Virol. 3, 34–43.
[44] Du, J., Bhattacharya, B., Ward, T.H. and Roy, P. (2014) Trafficking of bluetongue virus visualized by recovery of tetracysteine-tagged virion particles. J. Virol. 88, 12656–12668.
[45] Matsuo, E., Leon, E., Matthews, S.J. and Roy, P. (2014) Structure based modification of bluetongue virus helicase protein VP6 to produce a viable VP6-truncated BTV. Biochem. Biophys. Res. Commun. 451, 603–608.
[46] Boyce, M., Celma, C.C. and Roy, P. (2008) Development of reverse genetics systems for bluetongue virus: recovery of infectious virus from synthetic RNA transcripts. J. Virol. 82, 8339–8348.
[47] Boyce, M. and Roy, P. (2007) Recovery of infectious bluetongue virus from RNA. J. Virol. 81, 2179–2186.
[48] Kaname, Y., Celma, C.C., Kanai, Y. and Roy, P. (2013) Recovery of African horse sickness virus from synthetic RNA. J. Gen. Virol. 94, 2259–2265.
[49] Fontes, L.V.Q., Campos, G.S., Beck, P.A., Brandao, C.F.L. and Sardi, S.I. (2005) Precipitation of bovine rotavirus by polyethylen glycol (PEG) and its application to produce polyclonal and monoclonal antibodies. J. Virol. Methods 123, 147–153.
[50] Benavides, J., Mena, J.A., Cisneros-Ruiz, M., Ramirez, O.T., Palomares, L.A. and Rito-Palomares, M. (2006) Rotavirus-like particles primary recovery from insect cells in aqueous two-phase systems. J. Chromatogr. B Analyt. Technol. Biomed. Life Sci. 842, 48–57.
[51] Weiner, M.P., Costa, G.L., Schoettlin, W., Cline, J., Mathur, E. and Bauer, J.C. (1994) Site-directed mutagenesis of double-stranded DNA by the polymerase chain reaction. Gene 151, 119–123.
[52] Matsuo, E. et al. (2006) Characterization of HCV-like particles produced in a human hepatoma cell line by a recombinant baculovirus. Biochem. Biophys. Res. Commun. 340, 200–208.
[53] Savini, G. et al. (2011) Epizootic hemorrhagic disease. Res. Vet. Sci. 91, 1–17.
[54] Coetzer, J.A.W. and Guthrie, A.J. (2004) African horse sickness in: Infectious Diseases of Livestock (Coetzer, J.A.W. and Tustin, R.C., Eds.), pp. 1231–1246, Oxford University Press Southern Africa, Cape Town.
[55] Batten, C.A., Edwards, L., Bin-Tarif, A., Henstock, M.R. and Oura, C.A. (2011) Infection kinetics of epizootic haemorrhagic disease virus serotype 6 in Holstein–Friesian cattle. Vet. Microbiol. 154, 23–28.
[56] Aradaib, I.E., Sawyer, M.M. and Osburn, B.I. (1994) Experimental epizootic hemorrhagic disease virus infection in calves: virologic and serologic studies. J. Vet. Diagn. Invest. 6, 489–492.
[57] Abdy, M.J., Howerth, E.E. and Stallknecht, D.E. (1999) Experimental infection of calves with epizootic hemorrhagic disease virus. Am. J. Vet. Res. 60, 621–626.
[58] Bartenschlager, R., Kaul, A. and Sparacio, S. (2003) Replication of the hepatitis C virus in cell culture. Antiviral Res. 60, 91–102.
[59] Lohmann, V., Hoffmann, S., Herian, U., Penin, F. and Bartenschlager, R. (2003) Viral and cellular determinants of hepatitis C virus RNA replication in cell culture. J. Virol. 77, 3007–3019.
[60] Date, T. et al. (2007) An infectious and selectable full-length replicon system with hepatitis C virus JFH-1 strain. Hepatol. Res. 37, 433–443.
[61] Lindenbach, B.D. et al. (2005) Complete replication of hepatitis C virus in cell culture. Science 309, 623–626.
[62] Luking, A., Stahl, U. and Schmidt, U. (1998) The protein family of RNA helicases. Crit. Rev. Biochem. Mol. Biol. 33, 259–296.
[63] Matsuo, E. et al. (2011) Generation of replication-defective virus-based vaccines that confer full protection in sheep against virulent bluetongue virus challenge. J. Virol. 85, 10213–10221.
[64] Kar, A.K., Bhattacharya, B. and Roy, P. (2007) Bluetongue virus RNA binding protein NS2 is a modulator of viral replication and assembly. BMC Mol. Biol. 8, 4.
[65] Lymperopoulos, K., Noad, R., Tosi, S., Nethisinghe, S., Brierley, I. and Roy, P. (2006) Specific binding of bluetongue virus NS2 to different viral plus-strand RNAs. Virology 353, 17–26.
[66] Lymperopoulos, K., Wirblich, C., Brierley, I. and Roy, P. (2003) Sequence specificity in the interaction of bluetongue virus non-structural protein 2 (NS2) with viral RNA. J. Biol. Chem. 278, 31722–31730.
[67] Modrof, J., Lymperopoulos, K. and Roy, P. (2005) Phosphorylation of bluetongue virus nonstructural protein 2 is essential for formation of viral inclusion bodies. J. Virol. 79, 10023–10031.